Journal of Organometallic Chemistry 896 (2019) 194–206

Contents lists available at ScienceDirect

Journal of Organometallic Chemistry

journal homepage: www.elsevier.com/locate/jorganchem

Copper(II)-faciliated synthesis of substituted thioethers and 5-substituted 1*H*-tetrazoles: Experimental and theoretical studies

Samaresh Layek [a], Bhumika Agrahari [a], Shuvankar Dey [b], Rakesh Ganguly [c], Devendra D. Pathak [a, *]

[a] Department of Applied Chemistry, Indian Institute of Technology (ISM), Dhanbad, 826004, India
[b] Department of Chemistry, School of Sciences, Gujarat University, Ahmedabad, 380009, India
[c] Division of Chemistry & Biological Chemistry, Nanyang Technological University, Singapore, 639798

ARTICLE INFO

Article history:
Received 10 May 2019
Received in revised form
5 June 2019
Accepted 9 June 2019
Available online 15 June 2019

Keywords:
Copper(II) complex
Crystal structure
Homogeneous catalysis
Thioethers
Tetrazoles

ABSTRACT

Benzoylhydrazine based Schiff base-ligated two new copper(II) complexes, $[Cu(L^1)_2]$ **(1)** and $[Cu(L^2)_2]$ **(2)** were synthesized by the reaction of $Cu(CH_3COO)_2 \cdot H_2O$ with respective Schiff base ligand 1-[(4-nitrophenyl)ethylidene] benzohydrazide (HL^1) or 1-[(4-methoxyphenyl)ethylidene] benzohydrazide (HL^2). Both complexes were isolated as greenish solid and fully characterized by elemental analysis, FT-IR, EPR, thermo-gravimetric (TG) analysis and Cyclic Voltammetry. The molecular structures of both complexes have also been determined by single crystal X-ray crystallography, which confirmed the co-ordination of Schiff base ligands through N, O donor atoms and distorted square planar geometry around the Cu(II) ion. Both complexes were found to be good homogeneous catalysts for the synthesis of a wide range of substituted thioethers and 5-substituted 1*H*-tetrazoles in 92% and 93% yield, respectively, at a low catalyst loading (0.5 mol%). The bond angles and distances, as discerned from the DFT calculations, commusurated with the experimental findings. The energy difference between the HOMO and the LUMO, calculated from DFT studies, was found to be 5.645 eV and 6.459 eV for complex **1** and complex **2**, respectively. These results are in harmony with the observed higher catalytic activity of complex **1.**

© 2019 Elsevier B.V. All rights reserved.

1. Introduction

The miscellaneous applications of copper-based complexes have accentuated a great deal of interest in the field of catalysis [1], biology [2] and active pharmaceutical ingredients (API's) [3]. These complexes have been reported to catalyze a broad range of organic reactions [4]. Owing to the versatility of design and fine-tuning of these complexes, one can achieve an easy control over the reaction mechanism, rate and selectivity of the respective catalytic processes [5]. Copper-catalyzed coupling reactions are important tools for formation of carbon-heteroatom bonds [6]. Among the various copper-catalyzed coupling reactions, C–S and C–N bond forming reactions have gained much impetus due to their applications in the preparation of numerous important products in the field of pharmaceutical, biological, and material science [7].

Development of efficient methods for the C–S bond formation is a significant research theme of organic synthesis [8]. In this perception, transition metal-catalysed C–S cross-coupled thioethers have occupied a prominent role in organic synthesis [9]. Aryl and aryl alkyl thioethers are used as essential building blocks for many biologically and pharmaceutically active compounds such as, antibiotic (Gemmacin B) and HIV protease inhibitor agents (Nelfinavir). Diaryl thioether scaffolds are an intergral structural motif of several biologically important products, viz. Lissoclibadin 6, an antimicrobial agent, and AZD4407, a natural product-inspired drug molecules which acts as 5-lipoxygenase inhibitor. (Fig. 1) [10].

A perusal of the literature indicated that these thioethers were synthesised by the reaction of the corresponding Grignard reagent or arylboronic acid/aryl halide derivatives with a suitable electrophilic aryl sulfur reagent (thiols) in presence of a variety of palladium, copper, nickel, cobalt and other metal complexes [11,12]. Although spectacular success in these reactions were achieved using different catalysts, but all these methods suffer from one or other drawback such as, use of precious palladium precursor and an additional ligand, inert atmosphere, use of hazardous solvents, high catalyst loading, and prolong reaction time etc. [13].

The formation of C–N bond in aromatic compounds is another

* Corresponding author.
E-mail addresses: ddpathak@iitism.ac.in, ddpathak@yahoo.com (D.D. Pathak).

https://doi.org/10.1016/j.jorganchem.2019.06.008
0022-328X/© 2019 Elsevier B.V. All rights reserved.

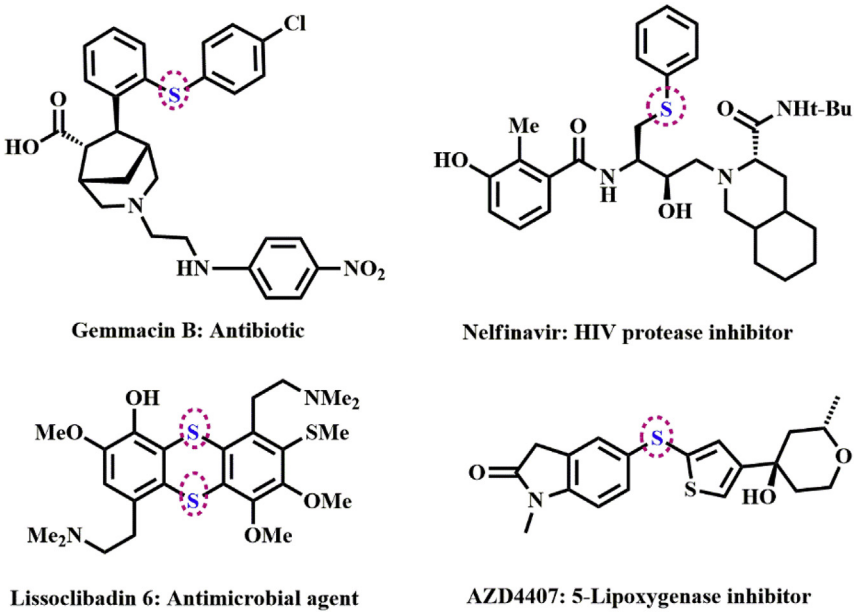

Fig. 1. Typical examples of biologically significant thioether.

powerful tool in the armoury of an organic chemist for the design of biological active molecules [14]. Tetrazoles are some of the most stable nitrogen rich heterocyclic compounds that have received bewildering range of applications in the field of coordination chemistry, organic synthesis, material science and medicinal chemistry as antiprotozoal, antihypertensive and antibiotic [15,16]. For instance, Valsartan and Losartan are the typical examples of anti-hypertive drugs and both contain tetrazole moiety as an integral part of their structure (Fig. 2) [17].

Owing to the versatile applications of numerous tetrazole derivatives, several methods for their synthesis have been documented [18]. The most convenient method involves a [3 + 2]-cycloaddition of organic nitriles to azides, which was first reported by Hantzsch et al., in 1901 [19]. As perusal of the literature reveals that many catalysts have been reported for the synthesis of tetrazoles [20–30]. Although different nitriles served as successful substrates for the synthesis of tetrazoles, majority of them are legitimately expensive, toxic and not readily available. Hence, the use of easily available, less toxic and cheap starting materials for efficient synthesis of 5-substituted 1*H*-tetrazoles is an attractive preposition. In view of the ease of availability, wide diversity, lower toxicity, and ease of handling of aldehydes compared with nitriles, the direct application of aldehydes for synthesis of 5-substituted 1*H*-tetrazole derivatives may be a highly attractive and worth investigating [31].

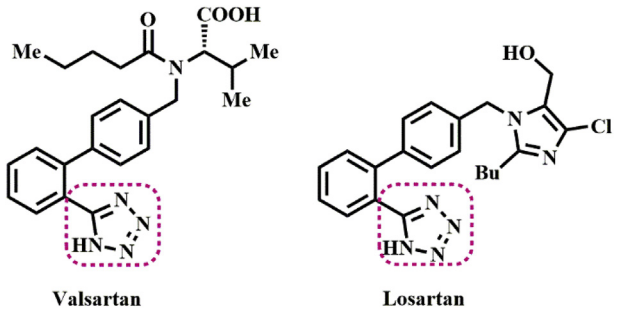

Fig. 2. Typical examples of biologically significant 1 *H*-tetrazoles.

In view of the easy synthesis and stability of Schiff base ligand derived copper(II) complexes and of our ongoing research interest on the synthesis, structural characterization and catalytic applications of transition metal complexes [32], we herein describe the synthesis of benzoylhydrazine based Schiff base ligated two new copper(II) complexes, namely $[Cu(L^1)_2]$ **(1)** and $[Cu(L^2)_2]$ **(2)**, and their catalytic activity towards the synthesis of diaryl sulphides *via* C–S bond formation from the reaction of a number of aryl halides and various thiophenols and in synthesis of 5-substituted 1*H*-tetrazoles from three component reaction of aldehyde, hydroxylamine hydrochloride and sodium azide.

2. Results and discussion

2.1. Synthesis and characterization of ligands and complexes

The preparation of benzoylhydrazone based Schiff base ligands (HL^1 & HL^2) and two new copper complexes of the type $[Cu(L^1/L^2)_2]$ is outlined in Scheme 1. Condensation of 4-nitroacetophenone and 4-methoxyacetophenone with benzoylhydrazine in 1:1 M ratio in ethanol under reflux lead to the formation of the N, O donor bidentate Schiff base ligands HL^1 and HL^2, respectively in 75–85% yield. These Schiff base ligands are stable, solids and can be stored without precautions. In general, HL^1 and HL^2 ligands are fully soluble in common organic solvent such as methanol, *N, N*-dimethyl formamide (DMF), dimethyl sulfoxide (DMSO) and sparingly soluble in dichloromethane (DCM), chloroform ($CHCl_3$), and ethanol etc. The reaction of the Schiff base ligands with copper acetate in 2:1 M ratio in methanol at room temperature for 12 h afforded the corresponding complexes, $[Cu(L^1)_2]$ **(1)** and $[Cu(L^2)_2]$ **(2)** in good yields. Both complexes were isolated as green block shaped crystals. Suitable single crystals for X-ray crystallography were grown over a period of few days on standing a concentrated solution of the complexes in DMF at room temperature.

2.2. FT-IR spectra of free ligands (HL^1 and HL^2) and complexes

FT-IR spectra of free ligands (HL^1 and HL^2), complexes **1** and **2** were recorded by use of KBr disc and their characteristic bands are

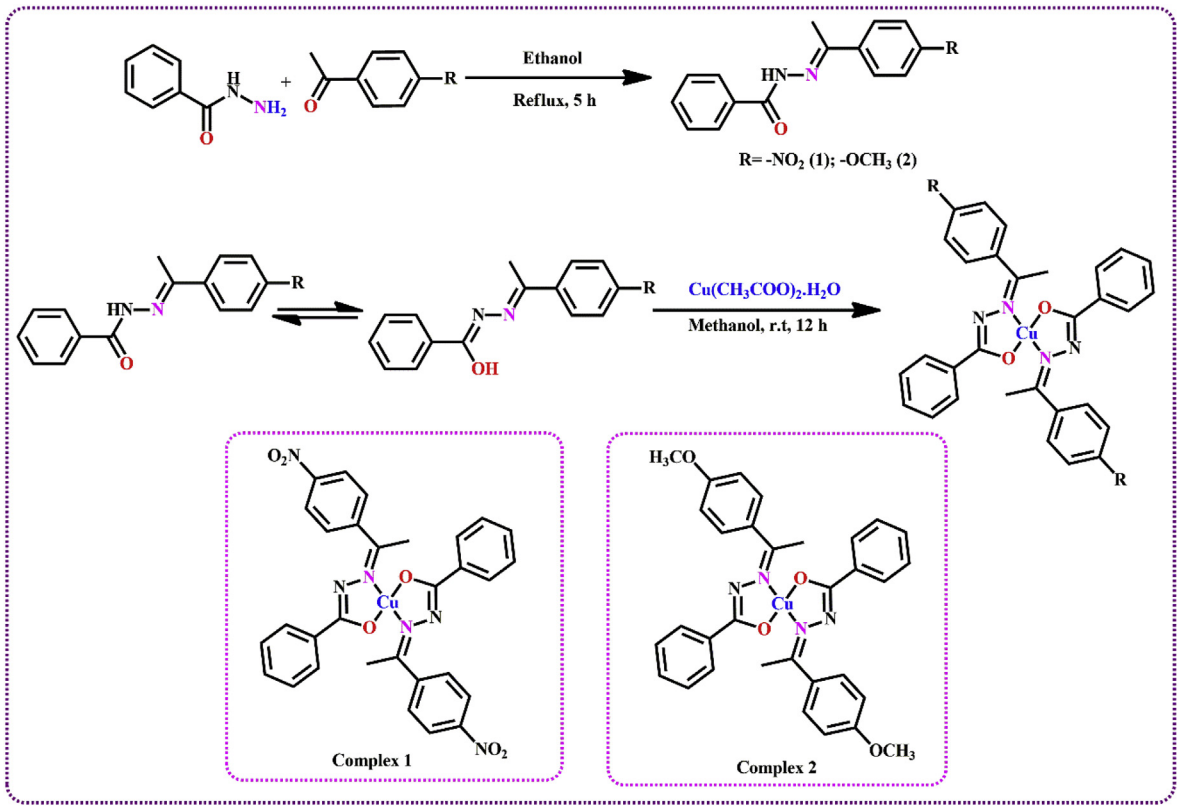

Scheme 1. Synthesis of Schiff base ligands and copper(II) complexes.

summarized in Table 1S and spectra are shown in Figs. S1–S4. The FT-IR spectra of the synthesized Schiff base ligand HL^1 and HL^2 exhibited a band at 3187 cm^{-1} and 3193 cm^{-1} respectively, due to νNH groups. Both ligands revealed a sharp band at 1667 cm^{-1} and 1643 cm^{-1}, respectively due to νC = O. The presence of νNH and νC = O clearly indicated that both ligand existed predominantly in keto form in the solid state. The FT-IR spectra of the ligand HL^1 and HL^2 also showed an intense band at around 1519 cm^{-1} and 1593 cm^{-1}, respectively due to the presence of azomethine group of Schiff base ligands. The FT-IR spectra of both copper(II) complexes **1** and **2** exhibited bands at 1511 cm^{-1} and 1591 cm^{-1} respectively, assignable to νC = N stretching frequency. A comparison of the FT-IR of the each ligand and their complexes clearly indicated that the C=N stretching frequency were shifted to lower wave number by 8 cm^{-1} and 16 cm^{-1} in complex **1** and complex **2**, respectively. The shifting of azomethine stretching frequency to lower wave number may be taken as evidence for the coordination of the nitrogen atom to the metal [33]. The disappearance of νNH and νC = O peaks and appearance of a peak at 572 cm^{-1} and 564 cm^{-1} (νCu-O) and 508 cm^{-1} and 514 cm^{-1} (νCu-N) in the FT-IR spectra of complex **1** and complex **2**, respectively supports the formation of complexes.

2.3. ^1H and ^{13}C NMR spectra of ligands

The ^1H and ^{13}C NMR spectra of HL^1 and HL^2 were recorded in DMSO-d_6 (Figs. S5–S8) and their spectral data are summarized in Table 2S. The ^1H NMR spectra of both ligands show a singlet at δ 10.97 and δ 10.67, due to presence of -N*H* proton. A singlet at δ 2.43 and δ 2.33 corresponds to aliphatic CH_3 protons of acetophenone moiety in HL^1 and HL^2, respectively. In ligand HL^2, an additional singlet at δ 3.80 is due to the presence of -OCH_3 protons of 4-methoxyacetophenone moiety. All aromatic protons appear in the range of δ 6.99–8.29. Both ligands show an intense peak at δ 3.55 and δ 3.55 may be due to the impurity in the solvent [34]. The ^{13}C NMR spectra of both ligands exhibited a signal at δ 164.97 and δ 164.04 corresponding to characteristic carbonyl (C=O) carbon of benzoylhydrazine moiety. The signal at δ 148.07 and δ 156.52 appeared due to presence of imine carbon (*C*=N) of ligand HL^1 and HL^2 respectively. The methyl carbon (-CH_3) of acetophenone moiety in both ligands showed a signal at δ 14.90 and δ 15.00. An additional signal in the ^{13}C NMR spectrum of HL^2 at δ 55.77 accounted to the aliphatic -OCH_3 carbons.

2.4. EPR spectrum of the complexes

The EPR spectrum of both complexes were recorded at room temperature and the spectra are shown in Fig. 3. Complex **1** displayed well resolved an isotropic behaviour with a sharp signal and without any hyperfine splitting having g_{iso} value of 2.0907, indicative of square planar Cu(II) geometry [35]. The EPR spectrum of complex **2** exhibits four well-defined anisotropic signals with hyperfine splitting which may be attributed to single electron interaction of copper(II) with nuclear spin I = 3/2 [36]. Analysis of the EPR spectrum of the complex **2**, $g_{||} = 2.392$, $g_{\perp} = 2.066$ and $A_{||=}$13 mT. Since $g_{||}$ and $g_{\perp}$ values are closer to 2 and observed $g_{||} > g_{\perp}$, it is concluded that the unpaired electron is located at dx^2-y^2 orbital having distorted square planar geometry for copper complex [37].

2.5. Thermogravimetric analysis (TGA) of the complexes

Thermogravimetric analysis (TGA) of the complexes was carried out in the temperature range of 30–800 °C with a 10 °C/min interval in nitrogen atmosphere (Fig. S9), in order to assess the

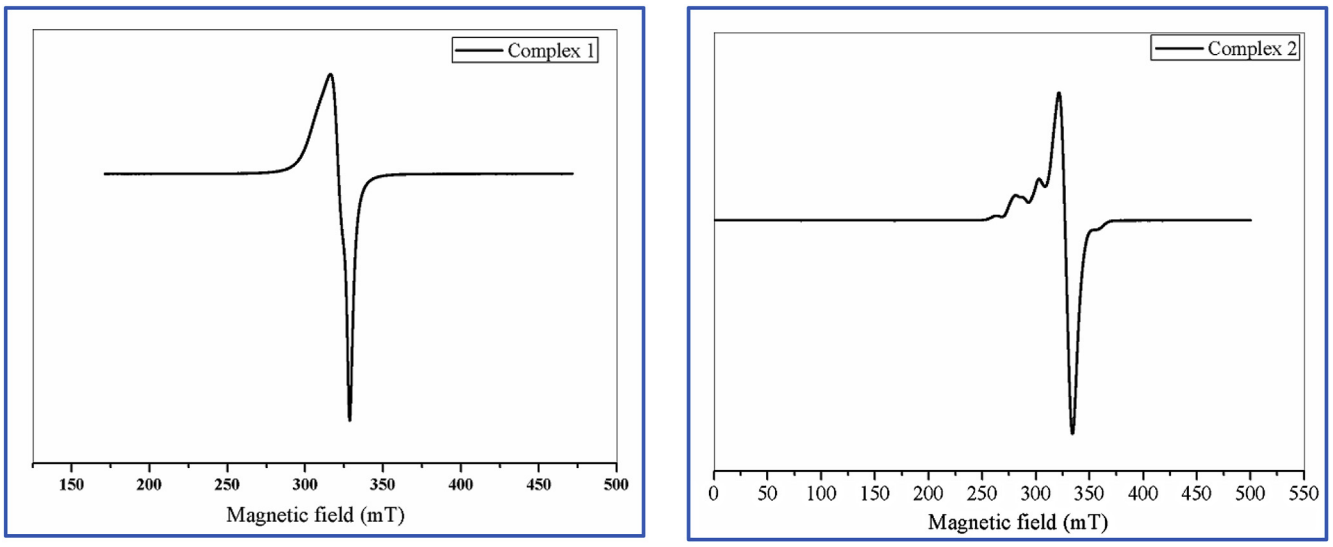

Fig. 3. EPR spectra of complex **1** & complex **2**.

stability and mode of decomposition of the complexes. The TGA thermograms indicated the absence of water molecule in both complexes. The complex **1** and **2** were found to be stable up to 220 °C and 202 °C, respectively. Above these temperatures, both complexes undergo decomposition in three well separated stages. In the first step, complex **1** shows a weight loss of 30.03% in the temperature range 220–320 °C and complex **2** shows a weight loss of 11.60% in the temperature range 202–315 °C. In the second stage, weight loss for complex **1** and complex **2** were observed by 16.92% and 45.07% within the temperature range 320–530 °C and 315–497 °C, respectively. The corresponding weight loss at this stage may be attributed to removal of nitro and methoxy groups of the corresponding complexes. In the third or final decomposition stage, the remaining organic moiety i.e. chelate part was eliminated in the temperature of beyond 500 °C.

2.6. Cyclic Voltammetry

To investigate the redox properties of Cu(II) complexes, the electrochemical behaviour of the Schiff base ligands (10^{-3} M) and their copper(II) complexes (10^{-3} M) were investigated by Cyclic Voltammetry (CV) technique using 0.1 M [nBu$_4$N][ClO$_4$] as a supporting electrolyte in DMF solvent at scan rate of 100 mV/S (Fig. 4). The Cyclic Voltammogram of the ligand 1 shows three reduction peaks at −1.49, −1.13 and −0.96 V vs. SCE. But in case of complex **1**, the metal based redox peak appeared at $E_{1/2} = -0.261$ V vs. SCE due to Cu^{II}/Cu^{I} redox couple. Along with the metal based redox process, two ligand centered reduction peaks also appeared at −1.74 and −1.17 V vs. SCE. In case of ligand **2**, the Cyclic Voltammogram shows two irreversible peaks at −2.07 and −1.84 V vs. SCE. Complex **2** shows one quasi reversible peak at $E_{1/2} = -0.41$ V vs. SCE due to Cu^{II}/Cu^{I} redox couple [38].

2.6.1. Single crystal X-ray studies

Diffraction quality crystals of both complexes, namely [Cu(L^1)$_2$] **(1)** and [Cu(L^2)$_2$] **(2)** were grown by slow evaporations of DMF solution of the complexes at room temperature and structures of both complexes was unambiguously confirmed by single crystal X-

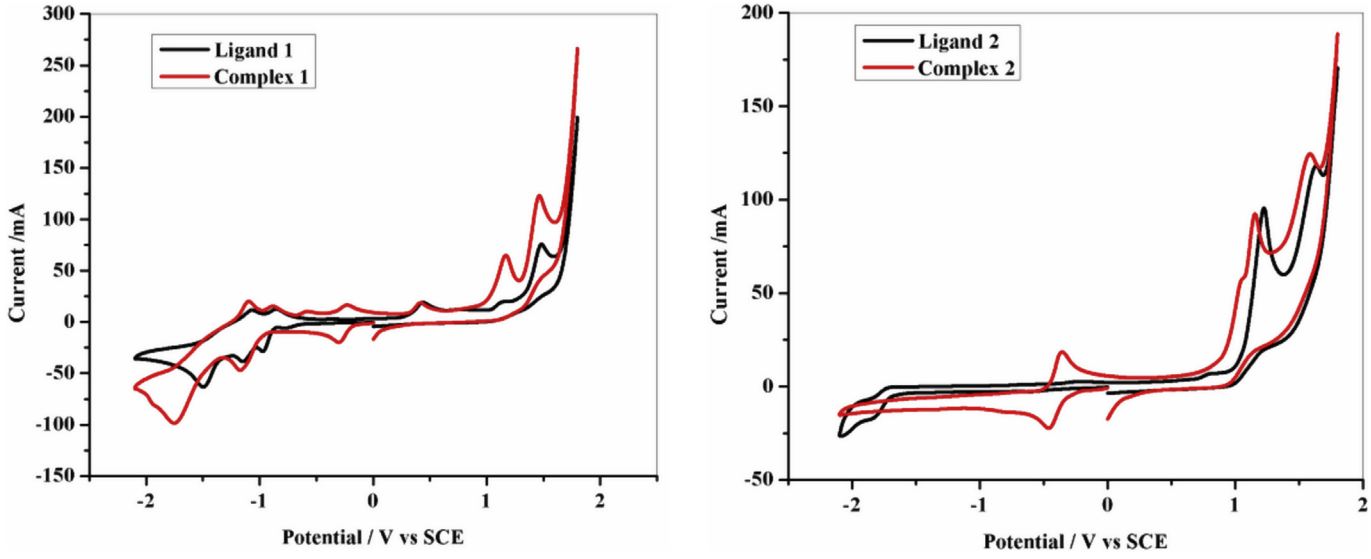

Fig. 4. Cyclic Voltammogram of the ligands and complexes at scan rates of 100 mV/s SCE *2.7.*

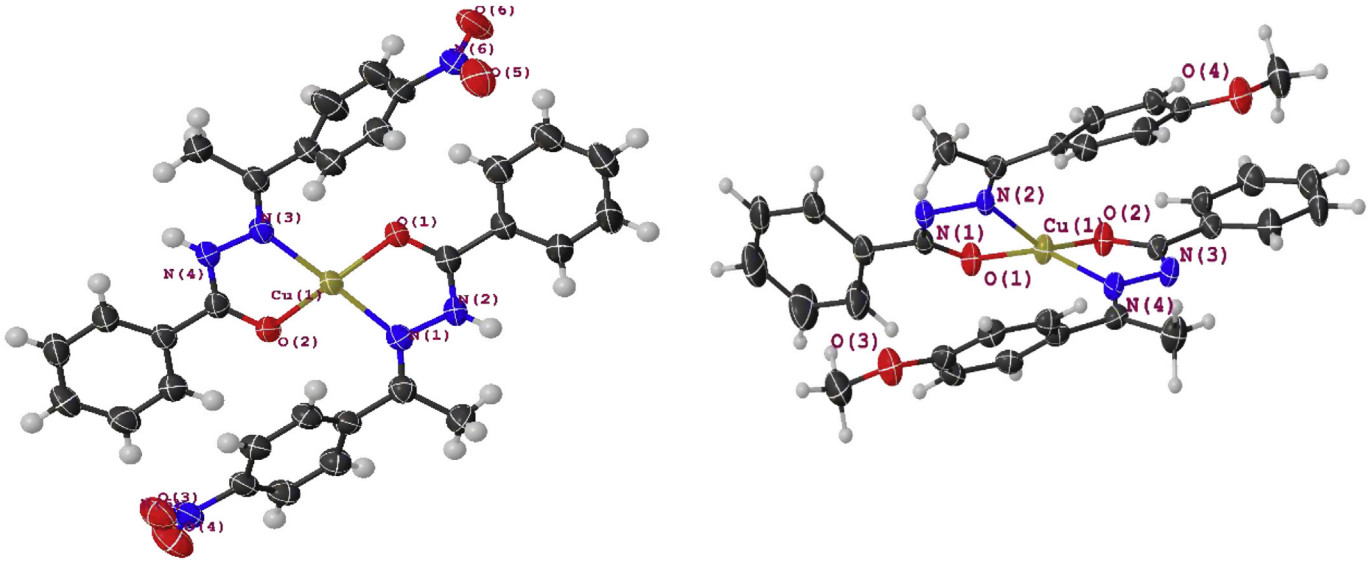

Fig. 5. ORTEP diagram of $[Cu(L^1)_2]$ (1) and $[Cu(L^2)_2]$ (2) complexes with the non C, H atoms labelling scheme (Thermal ellipsoids are drawn at the 50% probability level).

ray studies. The molecular structures (ORTEP Digrams) along with the non C, H atom numbering schemes are depicted in Fig. 5. The X-ray investigation exposes that both complexes crystallizes in monoclinic system, having space group P 21/n for complex **1** and P 21/c for complex **2**. Both complexes show monomeric square planar geometry around the metal center where the metal ion is four-coordinated by two imine N atoms and two benzoyl O atoms from two units of Schiff base ligands in a *trans*-position through creating two five-membered metallocycle with metal center. A summary of the crystallographic and refinement data of complexes is given in Table 1 and selected bond lengths and bond angles are also given in Table 3S. The complex **2** is slightly distorted from square planar geometry when compared to that of complex **1** as the O1—Cu1—O2, O1—Cu1—N4 and N(1)-Cu(1)-N(3) chelate bite angles of the complexes **1** and **2** are in the range of 83.7(2)°-95.2(2)°, 83.61(10)°-94.62(10)° and 174.6(2)°-174.88(11)°, respectively. The Cu—O bond distances in the range of 1.9038(18)-1.9199(18) Å in complex **2** are slightly longer than that of 1.8903(1)-1.8966(1) Å observed in complex **1**, while the Cu—N bond distances in the range of 1.955(2)-1.981(2) Å in complex **2** are slightly shorter than that of 2.030(1)-2.032(1) Å of complex **1**. This may be due to the electron withdrawing effect of the nitro substituent of the complex **1** [39]. Packing structure of complexes **1** and **2** is shown in ESI Fig. S10 and Fig. S11 respectively.

2.6.2. Catalytic studies

In continuation of our previous studies and research interest on transition metal catalysed organic reactions, we were interested in finding a simple and efficient method for the synthesis of diaryl sulphides *via* C—S coupling of thiols with various bromo- or iodo-

Table 1
Crystallographic and refinement data for $[Cu(L^1)_2]$ (**1**) and $[Cu(L^2)_2]$ (**2**) complexes.

Crystal data	Complex 1	Complex 2
CCDC deposition number	1585130	1585131
Chemical formula	$C_{30}H_{24}CuN_6O_6$	$C_{32}H_{30}CuN_4O_4$
Formula weight	628.09 g/mol	598.14 g/mol
Temperature	100(2) K	103(2) K
Wavelength	0.71073 Å	0.71073 Å
Crystal size	0.060 × 0.140 × 0.200 mm	0.160 × 0.240 × 0.300 mm
Crystal system	monoclinic	monoclinic
Space group	P 21/n	P 21/c
Unit cell dimensions	$a = 9.6565(3)$ Å $b = 9.6293(3)$ Å $c = 29.1154(8)$ Å $\alpha = 90°$; $\beta = 92.5730(10)°$; $\gamma = 90°$	$a = 13.3310(12)$ Å; $b = 15.2582(12)$ Å $c = 14.1779(12)$ Å; $\alpha = 90°$; $\beta = 97.088(2)°$; $\gamma = 90°$
Volume	2704.58(14) $Å^3$	2839.3(4) $Å^3$
Z	4	4
Density (calculated)	1.543 g/cm^3	1.399 g/cm^3
Absorption coefficient	0.866 mm^{-1}	0.814 mm^{-1}
F(000)	1292	1244
Reflections collected	48810	25402
Independent reflections	8601 [$R_{int} = 0.0406$]	5822 [$R_{int} = 0.0635$]
Goodness-of-fit on F^2	1.037	1.008
Final R indices	7058 data; $I > 2\sigma(I)$; R1 = 0.0392, w*R*2 = 0.0773	4045 data; $I > 2\sigma(I)$; R1 = 0.0392, w*R*2 = 0.0773
R.M.S. deviation from mean	0.068 $eÅ^{-3}$	0.063 $eÅ^{-3}$

benzenes and 5-substituted 1*H*-tetrazole *via* one-pot three component reaction of aldehyde, hydroxylamine hydrochloride and sodium azide using fully characterized new copper(II) complexes **1** and **2** as homogeneous catalysts (Scheme 2).

To explore the catalytic potential of the complexes **1** and **2** for C–S bond formation reaction, 4-methoxyiodobenzene and thiophenol were chosen as model substrates. To optimize the reaction conditions, a series of experiments were performed with variation of reaction parameters, such as solvent, base, temperature, time and catalyst loading (Table 2). Initially, the reaction was carried out between 4-methoxyiodobenzene (0.234 g, 1.0 mmol) and thiophenol (0.132 g, 1.2 mmol) in the presence of 0.2 mol % complex **1** as catalyst, K_2CO_3 (1.0 mmol) as base in ethylene glycol as solvent at 90 °C for 6 h under atmospheric conditions. In this case, the desired product was obtained in only 65% yield (Table 2, entry 1). It was further observed that increasing the catalyst loading up to 0.5 mol% increases the product yield from 65 to 92% under the same reaction conditions (Table 2, entry 2). Further increase in the catalyst loading beyond 0.5 mol% did not increase the product yield appreciably (Table 2, entry 3). Control experiments confirmed that no conversion occurred without catalyst (Table 2, entry 4). Having determined the best solvent for this C–S coupling reaction, we studied the influence of other solvents such as toluene, dimethylformamide (DMF), acetonitrile, water, ethanol and PEG-200 on the reaction system (Table 2, entries 5–10). Among various solvents, environmentally benign ethylene glycol was found to be most effective solvent at 90 °C for the titled coupling reaction (Table 2, entry 2) and no reaction was observed in water, because of catalyst insolubility (Table 2, entry 8). When the reaction temperature was lowered to 60 °C, the yield also decreased (Table 2, entry 11). Further increase in the reaction temperature did not affect the reaction yield (Table 2, entry 12). In addition, the effect of base on this coupling reaction was also studied by using various bases such as, K_2CO_3, KOH, NaOH, Et_3N etc. where K_2CO_3 was found to be the best base (Table 2, Entries 2 & 13–15). A comparative catalytic study was carried out involving both catalysts (complex **1** & **2**) towards the chosen C–S coupling reaction (Table 2, entries 2 & 16). Complex **1** achieved better catalytic performance than the complex **2** which may be related to electronic effects of the coordinated ligand in the complex. This result is consistent with the theortical calaculations carried out on both complexes.

After optimization of the reaction conditions, this catalytic protocol was applied to the synthesis of a wide range of diary sulfides from a variety of substituted aryl halides (iodo or bromo) and substituted thiols. All products were obtained in good to excellent yields (Table 3). It is evident from Table 3, that both electron-donating and electron-withdrawing groups in the aryl iodide moiety were effective in this process, providing the corresponding products in good to excellent yields (Table 3, entries 2–6). Aryl bromides were also found to be suitable substrates for this coupling reaction (Table 3, entries 9–10). The scope of the reaction was extended to a number of thiols having electron-rich groups, i.e. *p*-toluenethiol, neutral thiophenol (thiophenol), electron-deficient thiophenol i.e. 4-chloro benzenethiol and also to sterically hindered thiophenol, i.e. 2-aminothiophenol under the optimized conditions (Table 3). The coupling appears to be insensitive to the electronic properties of the substrates. All reactions of both electron-rich and electron-defficient thiophenols with substituted iodobenzene or bromobenzene proceeded smoothly (Table 3). The sterically hindered ortho-substituted thiophenol (2-aminothiol) underwent arylthiolation with 4-methyliodobenzene without any difficulty (Table 3, entry 6). It is noteworthy that, under optimized conditions, heteroaryl thiol, i.e. 2-mercaptobenzimidazole, also provided the expected product in good yield (Table 3, entry 8). This clearly indicated that catalyst poisioning did not occur with heteroaryl thiols. Unfortunately, our efforts to use aryl chloride substrates instead of iodo or bromo analoues, did not succeed (Table 3, entry 16) owing to the less reactivity of C–Cl bond due to higher bond energy. In comparison with other reported catalytic systems [12a-12f] for synthesis of diaryl sulphides, the present catalyst showed better catalytic performance in terms of yields, catalyst loading, reactions time, TON, TOF etc. as shown in Table 4.

Complexes **1** and **2** were also screened for their catalytic potential in the syntheses of 5-substituted 1*H*-tetrazole. In order to find the optimum conditions, the reaction of benzaldehyde with hydroxylamine and sodium azide was studied as a model reaction. For this reaction, the effect of solvents, the amounts of the catalyst and the temperature were studied (Table 5). The reaction was carried out in the presence of 0.2 mol % of complex **1** as catalyst, in DMF at 110 °C for 5 h. In this case, the desired product was obtained in only 60% yield (Table 5, entry 1). It was further observed that an increase in the catalyst loading from 0.2 mol % to 0.4 mol % and 0.5 mol %, the yield of product significantly increases to 85% and 91%, respectively under the same reaction conditions (Table 5, entries 2–3). Further, no improvement in yield was noted when the catalyst loading was increased to 0.8 mol % (Table 5, entry 4). After optimization of the catalyst loading, the effect of solvents in the reaction was also investigated using different solvents such as ethylene glycol, DMSO, ethanol, methanol, H_2O etc. (Table 5, entries 5–10). DMF was found to be the most suitable solvent affording the maximum yield (91%) of the product. We noted the formation of oxime only, when the reaction was performed in methanol or ethanol (Table 5, entries 8–9). It was found that temperature has a profound effect on synthesis of 5-substituted 1*H*-tetrazoles. In the model reaction, the synthesis of 1*H*-tetrazoles was also conducted at different temperatures ranging from 80 °C to 130 °C (Table 5, entries 11–13). In presence of complex **2** as catalyst, there was afforded only 78% in yield of the product (Table 5, entry 14).

In order to extend the scope of the reaction, various aldehydes were examined under the optimized conditions and the results are summarized in Table 6. As demonstrated in Table 6, this protocol is rather general for a wide range of electron-withdrawing as well as

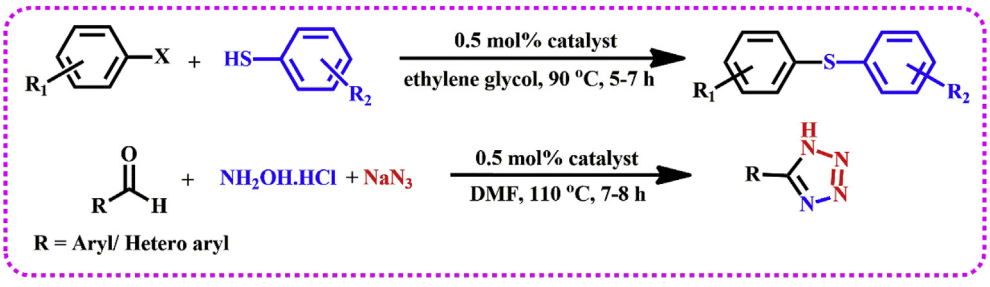

Scheme 2. Application of complex **1** and **2** for synthesis of substituted thioethers and 5-substituted 1*H*- tetrazoles.

Table 2
Optimization of the C–S coupling reaction to synthesized diaryl sulphides[a].

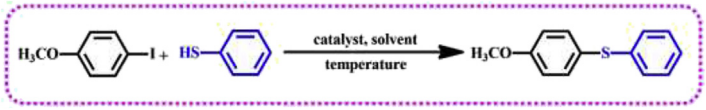

Entry	Catalyst	Catalyst loading (mol %)	Solvent	Base	Temp (°C)	Yield (%)[b]
1	Complex 1	0.2	Ethylene glycol	K_2CO_3	90	65
2	Complex 1	0.5	Ethylene glycol	K_2CO_3	90	92
3	Complex 1	0.8	Ethylene glycol	K_2CO_3	90	92
4	–	–	Ethylene glycol	K_2CO_3	90	n.r.
5	Complex 1	0.5	Toluene	K_2CO_3	90	47
6	Complex 1	0.5	DMF	K_2CO_3	90	45
7	Complex 1	0.5	CH_3CN	K_2CO_3	80	55
8	Complex 1	0.5	H_2O	K_2CO_3	90	n.r.
9	Complex 1	0.5	Ethanol	K_2CO_3	80	35
10	Complex 1	0.5	PEG-200	K_2CO_3	90	82
11	Complex 1	0.5	Ethylene glycol	K_2CO_3	60	75
12	Complex 1	0.5	Ethylene glycol	K_2CO_3	120	92
13	Complex 1	0.5	Ethylene glycol	Et_3N	90	75
14	Complex 1	0.5	Ethylene glycol	KOH	90	55
15	Complex 1	0.5	Ethylene glycol	NaOH	90	58
16	Complex 2	0.5	Ethylene glycol	K_2CO_3	90	83

n.r. = no reaction.
[a] Reaction condition: Aryl halide (1.0 mmol), Thiol (1.2 mmol), base (1.0 mmol) for 6 h.
[b] Isolated yields after column chromatography.

electron-donating aromatic aldehydes and afforded good to excellent yields (Table 6, entries 2–11). However aldehydes containing electron-withdrawing groups (Cl, Br, NO_2, $COCH_3$) gave products in better yields than those containing electron-donating groups (CH_3, OCH_3, OH) (Table 6). Steric hindrance on substrates is also an important parameter affecting the yield of the products. The *para*- and *meta*-substituted aldehydes resulted in good yield as compared to substituent at *ortho*-position may be due to steric effect. For instance, time and yield of the reaction for 3-nitrobenzaldehyde, 4-nitrobenzaldehyde, 3-bromobenzaldehyde, 4-bromobenzaldehyde, 2-hydroxybenzaldehyde, 4-hydroxy- benzaldehyde show this fact (Table 6, entries 4,8; 6,7; 10,11). The reaction of terepthaldehyde with one equivalent of other reactants afforded the corresponding tetrazole product, 4-(1*H*-tetrazol-5-yl)benzaldehyde in good yield (Table 6, entry 12). Heterocyclic aldehydes such as 2-thiophene-carboxaldehyde and 2-furancarboxaldehyde also underwent this three component reaction smoothly to afford corresponding tetrazoles products in good yields (Table 6, entries 13–14). Isolated products were fully characterized by standard spectroscopic methods. A comparison of the activities of complex **1** with some of the reported catalysts [31a-d] for the synthesis of 5-substituted 1*H*-tetrazoles showed that complex **1** has better catalytic activity compared to the other in terms of yields, catalyst loading, reactions time, TON, TOF etc. as shown in Table 7. The enhanced catalytic activity using copper(II) complexes may be due to the N, O-donor Schiff base ligands which increases the Lewis acidity and stability of the copper(II) catalysts and facilitate the reactions smoothly. Among the two, complex **1** exhibited better catalytic activity than the complex **2,** which may be related to electronic effects of the coordinated ligand in the complex. The complex **1** contains an electron withdrawing $-NO_2$ group which presumably renders the metal center more electron deficient (better Lewis acid) and showed higher catalytic activity. This result is also consistent with the theortical calaculations carried out on both complexes.

Based on the previous reports [30a,40] and our observations, a plausible reaction mechanism for the synthesis of 5-substituted 1*H*-tetrazole is represented in Scheme 3. It is proposed that at first, Cu(II) coordinates with oxygen of aldehyde to increases the electrophilicity of aldehyde [**I**]. After that the hydroxylamine attacks the carbonyl carbon of aldehydes to form oxime [**III**]. The oxime undergoes rearrangement followed by exclusion of water to afford the corresponding intermediate nitrile [**IV**]. The [3 + 2]-cycloaddition between the pre-coordinated nitrogen atom of the C≡N bond (intermediate [**IV**]) with azide ion takes place readily to form the intermediate [**VI**]. Protonolysis of the intermediate [**VI**] by 2 (N) HCl produce more stable desired product, 5-substituted 1*H*-tetrazole as white solid.

2.6.3. DFT study

To gain insight into the reactivity, vibrational attributions and absorption behaviour of the ligands as well as the corresponding complexes, the Density Functional Theory (DFT) and Time Dependent Density Functional Theory (TD-DFT) have been performed. After carefully observing the optimized structure of both the complexes, we compare them with the experimentally obtained data from single crystal XRD. A detailed comparison of the theoretical and experimental bond length and bond angle data are given in Table 4S. One can easily observe close resemblances between the two data. It is concluded from comparison of the optimized structures of both the complexes, that in the case of Complex **1**, unsubstituted phenyl ring was coplanar with Cu^{+2} forming a perfect square planer complex although the nitro substituted phenyl rings was tilted by about 120°. But, Complex **2** was devoid of such planarity and owing to the distorted structure.

An analysis of lowest energy configurations and frontier orbitals leads to qualitative insight towards the reactivity and optical responses of the complexes. The HOMO-LUMO energy gap of a complex influences in its chemical reactivity [41]. Larger the gap implies high kinetic stability and low chemical reactivity as it is energetically unfavorable to add electron to high lying LUMO or to extract an electron from low lying HOMO [42]. The d-orbital of Cu(II) interacting with the p-orbitals of oxygen and nitrogen atoms constitute these FMOs.

The HOMO energies of both the complexes were found nearer to each other and positioned primarily over Cu as well as unsubstituted benzene rings. The substituted (nitro or methoxy) benzene rings have only small share of these HOMOs (Fig. 6). On the other

Table 3
Copper(II)-catalyzed synthesis of diaryl sulphides[a].

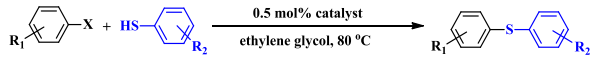

Entry	Aryl halide	Thiols	Product	Time (h)	Yields (%)[b]
1			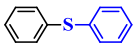	6	90
2			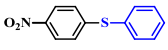	6	91
3			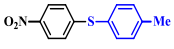	6	92
4			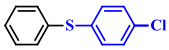	6	91
5	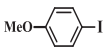		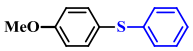	6	92
6			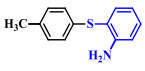	7	90
7			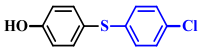	6	91
8		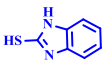	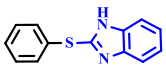	7	88
9			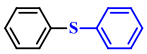	7	86
10	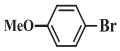	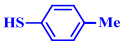	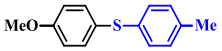	7	83
11		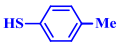	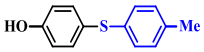	6	90
12	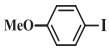	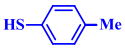	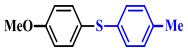	6	89
13		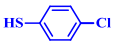	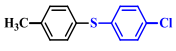	6	91
14				7	90
15				6	91
16				12	trace

[a] Reaction condition: Aryl halide (1.0 mmol), Thiol (1.2 mmol), K_2CO_3 (1.0 mmol).
[b] Isolated yields after column chromatography.

Table 4
A comparison study with some of the reported catalysts for the synthesis of diaryl sulphides.

Entry	Catalyst	Reaction conditions	Yields (%)	TON	TOF (h^{-1})	Ref.
1	10 mol% $FeCl_3$, 20 mol% DMEDA	Toluene/Na^tOBu/135 °C/24 h	91	9.1	0.38	[12a]
2	10 mol% $In(OTf)_3$, 20 mol% DMEDA	DMSO/KOH/135 °C/24 h	96	9.6	0.40	[12b]
3	10 mol% $Ni(OAc)_2$, 5 mol% Ipr	DMF/Na^tOBu/70 °C/12 h	92	9.2	0.77	[12c]
4	1 mol% $Pd(OAc)_2$, 1.2 mol% N-amido imidazolium salts	DMSO/Na^tOBu/80 °C/12 h	95	95	7.90	[12d]
5	20 mg Cu-grafted furfural funtionalised mesoporous silica	DMF/K_2CO_3/110 °C/12 h	85.2	–	–	[12e]
6	10 mol% I Mess-Cu-Cl	Toluene/Li^tOBu/120 °C/6 h	82	8.2	1.40	[12f]
7	0.5 mol% Copper(II) Schiff base (Complex 1)	Ethylene glycol/K_2CO_3/90 °C/6 h	90	180	30.0	*This work*

hand, Complex **1** LUMO which is primarily localized over the (-NO_2) substituted aromatic ring, acquires lower energy as compared to Complex **2**, reduces the band gap between HOMO and LUMO. Consequently, Complex **1** obtained significantly lower energy gap compared to Complex **2**, Which eventually ascertains the reactivity of Complex **1** is higher than Complex **2**. There is also a good match between experimentally observed and calculated distances for Cu–O and Cu–N bonds. The calculated and experimentally found

Table 5
Optimization of the reaction condition for the synthesis of 5-substituted 1*H*-tetrazole.[a].

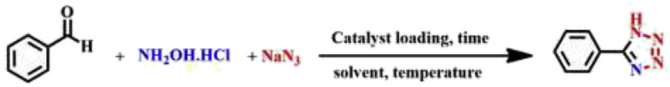

Entry	Catalyst	Catalyst loading (mol %)	Solvent	Temp. (° C)	Time (h)	Yields (%)[b]
1	Complex 1	0.2	DMF	110	5	60
2	Complex 1	0.4	DMF	110	7	85
3	Complex 1	0.5	DMF	110	7	91
4	Complex 1	0.8	DMF	110	7	92
5	Complex 1	0.5	DMF	110	9	92
6	Complex 1	0.5	DMSO	110	7	86
7	Complex 1	0.5	Ethylene glycol	110	7	45
8	Complex 1	0.5	Ethanol	110	7	n.r.
9	Complex 1	0.5	Methanol	110	7	n.r.
10	Complex 1	0.5	H_2O	110	7	n.r.
11	Complex 1	0.5	DMF	80	7	75
12	Complex 1	0.5	DMF	100	7	78
13	Complex 1	0.5	DMF	130	7	92
14	Complex 2	0.5	DMF	110	7	78
15	–	–	DMF	110	18	n.r.

[a] Reaction condition: Benzaldehyde (1 mmol), hydroxylamine hydrochloride (1.2 mmol), sodium azide (1.5 mmol), Solvent, catalyst.
[b] Isolated yields; n.r. = no reaction.

bond angles are also very close (Table 4S).

2.6.4. Molecular ESP calculation

The Electrostatic potential (ESP) has a unique role in the prediction and analysis of molecular recognition and is often helpful in demonstrating non-covalent molecular interaction properties [43]. The electrostatic potential surface of any molecule or complex is influenced by the charge density distribution. By employing the ESP surface, we can determine the spatial regions in the molecular structures at which point the molecular electrostatic potential is negative or positive [44]. The ESP surface visualize charged regions of a molecule and is qualitatively useful in the analysis of catalytic activity of a compound. Three-dimensional plots of the molecular electrostatic potentials of the ligands are illustrated in Fig. S12. The negative ESP regions are indicated in red, and the positive regions in blue. Potential is coded in the following order: red < orange < yellow < green < blue. Both the ligands have positive potential over aliphatic region and hydrogen atoms due to low electron density and lower electronegativity respectively. The most negative ESP region (shown in dark red), is located around carbonyl oxygen and its surrounding atoms. This large negative value is due to the lone pair of electrons on oxygen. These negative regions can be easily attracted by the positive potential regions of the metal ions and form strong complex. More the negative charge over the surface higher the possibility of catalytic reaction. Similarly, in case of complex (Fig. 7), metal ion and aliphatic region gains positive potential which arises from positive charge over metal and low electron density on these regions. The most positive potential area (show in dark blue) is located over the surface of metal ion, where the global maximum point is located.

3. Conclusions

In summary, hydrazone based N- and O- donor bidentate Schiff base-ligated two new copper(II) complexes, $[Cu(L^1)_2]$ **(1)** and $[Cu(L^2)_2]$ **(2)** were synthesized by the reactions of $Cu(CH_3COO)_2 \cdot H_2O$ with Schiff base ligand 1-(4-nitrophenyl)ethylidene) benzohydrazonic acid (HL^1) and 1-(4-methoxyphenyl)ethylidene) benzohydrazonic acid (HL^2), respectively. Both complexes were fully characterized using elemental analysis, FT-IR, EPR, thermogravimetric (TG) analysis and Cyclic Voltammetry. The single crystal X-ray diffraction studies revealed the bidentate chelation of these ligands to the metal center through N- and O-donor atoms and a distorted square planar geometry around the Cu(II) metal ion. The catalytic potential of both complexes was demonstrated in the synthesis of a series of substituted thioethers and 5-substituted 1*H*-tetrazoles. Complex **1** was found to be better catalyst than the complex **2**, and the maximum yield was obtained up to 92% for substituted thioethers and 93% for 5-substituted 1*H*-tetrazoles. The results of DFT calculations are consistent with the experimental bond lengths/bond angles. The HOMO-LUMO energy difference calculated from the DFT is lower for complex **1** than for complex **2.** This theortical observation augers well for the higher catalytic acitivity displayed by complex **1**. The ease of synthesis, air- and moisture-insensitivity, and good to excellent catalytic activities of the newly reported catalysts are some of the key features of the present methodology which may capture wide attention of numerous researchers and scientists in future.

4. Experimental section

4.1. Materials and physical measurements

All reagents and solvents for the synthesis and analysis were commercially available and used as received without further purification. The FT-IR spectra were recorded on a PerkinElmer Spectrometer (Model: Cary 660) in the range of 400–4000 cm^{-1} using KBr pellets in which MCT used as a detector with scan number 20, and resolution 4 cm^{-1}. The NMR spectra of complexes were recorded in $CDCl_3$/DMSO-d_6 on a Bruker 75 AvIII HD-400 MHz spectrometer using TMS as the internal standard.

4.2. General procedure for the synthesis of ligands HL^1 and HL^2

In a 25 ml round-bottomed flask, ethanolic solutions (5 ml) of benzoylhydrazine (1.0 mmol) and substituted acetophenone (R = 4-NO_2 or 4-OCH_3) (1.0 mmol) were stirred under reflux at 80 °C temperature in ethanol (5 ml) for 8 h. Upon cooling to 25 °C, precipitate was formed from the reaction mixture. After this, solid was filtered, washed with cold ethanol and dried vacuum over anhydrous $CaCl_2$.

Table 6
Cu(II)-catalyzed synthesis of 5-substituted 1*H*-tetrazoles form various aldehydes[a].

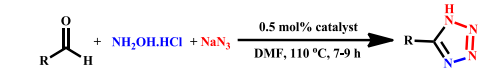

R = Aryl/ Hetero aryl

Entry	Aldehyde	Product	Time (h)	Yield (%)[b]	M.P (Exp./Lit.) (°C)
1	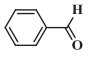	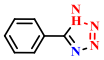	7	91	214-216/213-214
2	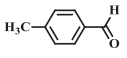	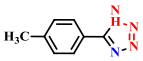	7	89	250-251/251-252
3	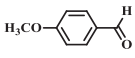	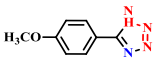	8	90	232-233/231-233
4	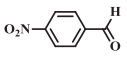	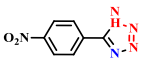	8	92	217-218/219-221
5	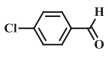	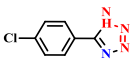	7	93	251-253/252-253
6	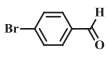	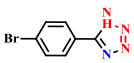	8	91	262-263/263-265
7		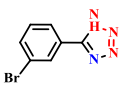	9	89	155-156/154-155
8	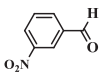	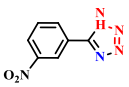	9	87	152-154/154-156
9	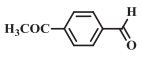	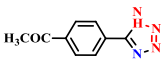	8	91	173-175/174-176
10	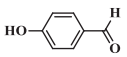	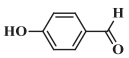	7	89	233-234/234-235
11		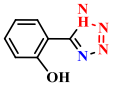	9	86	223-224/224-225
12	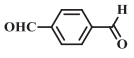	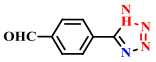	7	83	187-188/184-185
13		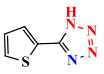	8	90	203-205/205-206
14		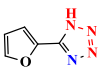	8	91	197-198/199-201

[a] Reaction condition: Aldehyde (1 mmol), hydroxylamine hydrochloride (1.2 mmol), sodium azide (1.5 mmol).
[b] Isolated yields.

Table 7
A comparison study with some of the reported catalysts for the synthesis of 5-phenyl-1*H*-tetrazole from benzaldehyde.

Entry	Catalyst	Reaction conditions	Yields (%)	TON	TOF (h^{-1})	Ref.
1	10 mol% $CuNO_3 \cdot 3H_2O$	DMSO/120 °C/24 h	78	7.8	0.33	[31a]
2	20 mol% $Cu(OAc)_2$	DMF/120 °C/12 h	96	4.8	0.4	[31b]
3	30 mg Cu-MCM-41	DMF/140 °C/12 h	90	–	–	[31c]
4	30 mg Nano-Cu_2O-MFR	DMF/100 °C/8 h	92	–	–	[31d]
5	0.5 mol% Copper(II) Schiff base (Complex **1**)	DMF/110 °C/7 h	91	182	26	*This work*

4.2.1. Schiff base ligand 1-[(4-nitrophenyl)ethylidene] benzohydrazide (HL^1)

Benzoylhydrazine (0.136 g, 1.0 mmol), 4-nitro acetophenone (0.165 g, 1.0 mmol), and ethanol (10 ml) afforded the title compound as a light yellow crystalline solid. Yield: 0.246 g, 87%, m.p = 202 °C; ^{1}H NMR (DMSO-d_6, 25 °C, 400 MHz): δ 10.97 (s, 1H, N*H*), 8.28 (d, 2H, Ar *H*), 8.10 (s, 2H, Ar *H*), 7.89 (s, 2H, Ar *H*), 7.60 (t, 1H, Ar *H*), 7.51–7.54 (m, 2H, Ar *H*), 2.43 (s, 3H, CC*H*$_3$); ^{13}C NMR (DMSO-d_6, 25 °C, 100 MHz): 164.97 (-NHC=O), 152.53 (Ar *C* adjacent to NO_2 group), 148.07 (*C*=N), 144.82 (Ar *C*), 134.30 (Ar *C*), 132.18 (Ar *C*), 128.82 (Ar *C*), 128.02 (Ar *C*), 124.11 (Ar *C*), 14.90 (-*C*H$_3$); Selected FT-IR (KBr), cm^{-1}: 3187 (νNH), 1667 (νC = O), 1583 (ν

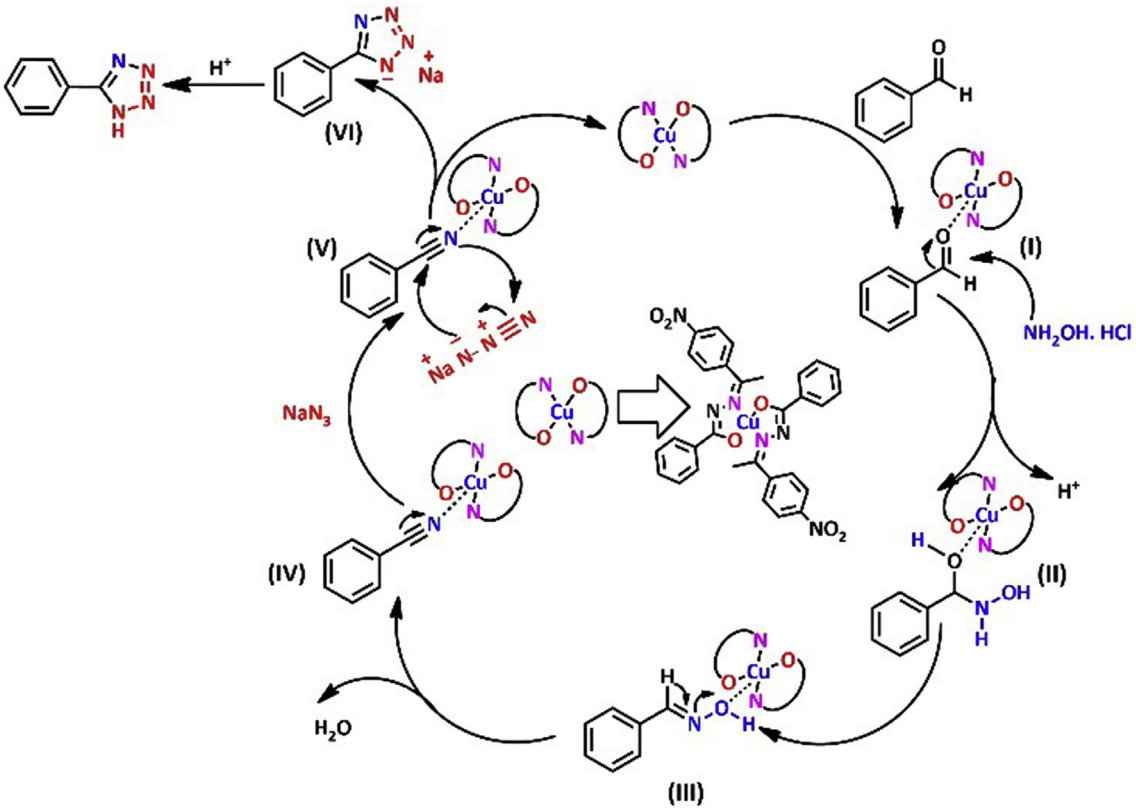

Scheme 3. Plausible mechanism for the synthesis of 5-substituted 1*H*-tetrazoles.

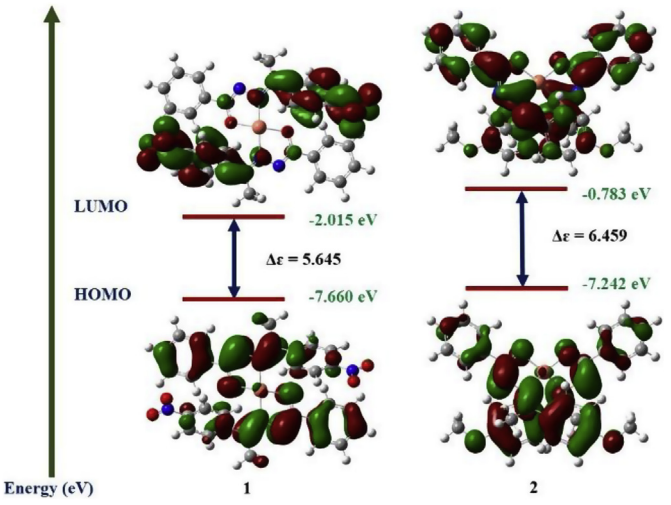

Fig. 6. Frontier molecular orbital diagrams of complex **1** and **2**.

N=O),1519 (ν C=N).

4.2.2. Schiff base ligand 1-[(4-methoxyphenyl)ethylidene] benzohydrazide (HL^2)

Benzoylhydrazine (0.136 g, 1.0 mmol), 4-methoxy acetophenone (0.150 g, 1.0 mmol), and ethanol (10 ml) afforded the title compound as off white crystalline solid. Yield: 0.225 g, 83%, m.p = 142 °C, ^{1}H NMR (DMSO-d_6, 25 °C, 400 MHz): δ 10.69 (s, 1H, N*H*), 7.85 (d, 4H, Ar *H*), 7.56 (d, 1H, Ar *H*), 7.51 (t, 2H, Ar *H*), 6.99 (d, 2H, Ar *H*), 3.80 (s, 3H, OC*H*$_3$), 2.33 (s, 3H, CC*H*$_3$); ^{13}C NMR (DMSO-d_6, 25 °C, 100 MHz): δ 164.06 (-NHC=O), 160.96 (Ar *C* adjacent to −OCH$_3$ group), 156.52 (*C*=N), 134.58 (Ar *C*), 131.12(Ar *C*), 128.84 (Ar *C*), 128.31 (Ar *C*), 114.50 (Ar *C*), 55.77 (-O*C*H$_3$), 15.00 (-*C*H$_3$); Selected FTIR (KBr), cm^{-1}: 3193 ν(N−H), 1643 ν(C=O), 1607 ν(C=N), 1539 ν(C=C).

4.3. Synthesis of copper(II) complexes

A methanolic solution of Cu(CH$_3$COO)$_2$. H$_2$O (0.5 mmol) was added drop-wise to a methanolic suspension (5 mL) of the HL^1 and HL^2 Schiff base ligand (1.0 mmol) separately, at room temperature. The reaction mixture was stirred for 12 h at room temperature to give greenish precipitate which was filtered, washed with cold methanol and dried vacuum over anhydrous CaCl$_2$. The precipitate was re-crystallized from DMF. Suitable single crystals for X-ray crystallography were grown over a period of few days from a concentrated solution of the complex in DMF.

Complex **1** [Cu(L^1)$_2$]: Yield: 0.553 g, 88%, Anal. Calc. for $C_{30}H_{24}CuN_6O_6$: C, 57.64; H, 3.75; N, 13.56. Found: C, 57.37; H, 3.85; N, 13.38; FTIR (KBr), cm^{-1}: 2857–2931 ν (CH$_2$), 1585 ν (N=O), 1511 ν (C=N), 572 ν (Cu−O), 508 ν (Cu−N); g_{iso} = 2.0907.

Complex **2** [Cu(L^2)$_2$]: Yield: 0.508 g, 85%, Anal. Calc. for $C_{32}H_{30}CuN_4O_4$: C, 64.45; H, 4.92; N, 9.30. Found: C, 64.26; H, 5.06; N, 9.37; FTIR (KBr), cm^{-1}: 2812–2925 ν(CH$_2$), 1591 ν(C=N), 1479 ν(C=C$_{ring}$), 564 ν(Cu−O), 514 ν(Cu−N); $g_{||}$ = 2.392, $g_{\perp}$ = 2.066 and $A_{||}$=13 mT.

4.4. General procedure for the synthesis of thioethers

A mixture of aryl halide (1.0 mmol), thiophenol (1.2 mmol), 0.5 mol % Cu(II) catalyst and K$_2$CO$_3$ (1.2 mmol) was stirred at 90 °C in ethylene glycol. The progress of the reaction was monitored by TLC. After the completion of the reaction, the reaction mixture was

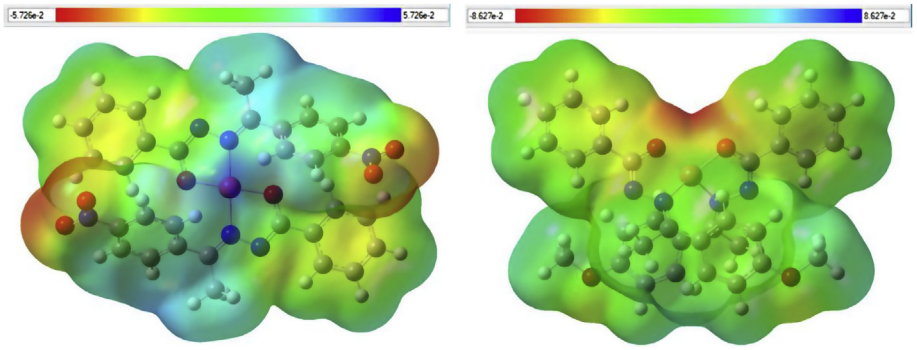

Fig. 7. Electrostatic potential (ESP) mapping of Complex 1 & 2.

cooled to room temperature and treated with water (3 ml) and ethylacetate (10 ml). The organic and aqueous layers were then separated and the aqueous layer was extracted with ethyl acetate (5 ml) for three times and dried with Na_2SO_4. The solvent was evaporated under vacuum to give crude product which was purified by coloum chromatography using petroleum ether/ethyl acetate as eluent. The spectra and physical properties of products were compared to those reported in the literature (Figs. S13–S25).

4.5. General procedure for the synthesis of 5-substituted 1H-tetrazole derivatives

A mixture of aldehyde (1.0 mmol), hydroxylamine hydrochloride (1.2 mmol) sodium azide (1.5 mmol), catalyst and DMF (3 mL) were taken in a 25 mL round bottomed flask and heated at 110 °C. After completion of the reaction (observed on TLC; petroleum ether: ethylacetate, 7:3), the reaction mixture was cooled to room temperature. After that 2 (N) HCl (10 ml) added to the solution and corresponding tetrazoles extracted with ethyl acetate (2 × 10 ml). The resultant organic layer was washed with distilled water and dried over sodium sulphate. The solvent removed under reduced pressure to give crude product which was purified by column chromatography by using petroleum ether/ethyl acetate as an eluent. The products were confirmed by melting point and NMR spectroscopic technique (Figs. S26–S39).

4.6. Crystallographic studies

Diffraction quality crystals of the complexes (**1** and **2**) were grownup over a period of few days from a concentrated solution of the complex in DMF and the structure of the complexes have been illuminated by single-crystal X-ray diffraction. The X-ray diffraction intensity data were measured at 103 K with a Bruker Kappa diffractometer equipped with a CCD detector, employing Mo K α radiation (λ = 0.71073 Å), with the SMART suite of programs [45]. All data were processed and corrected for Lorentz and polarization effects with SAINT and for absorption effects with SADABS [46]. Structural solution and refinement were carried out with the SHELXTL suite of programs [47]. The structures were refined (weighted least squares refinement on F^2) to convergence. All the non-hydrogen atoms in all the compounds were refined anisotropically till convergence is reached. A summary of the crystallographic and refinement data of these two copper complexes are given in Table 1.

4.7. Computational study

Geometry optimization and initial DFT calculations of both the ligand (L_1, L_2) were performed using Becke's three parametrized Lee-Yang-Parr (B3LYP) exchange-correlation function of Gaussian 09 package. The other calculations including single point energy of the complexes viz. Complex 1 and complex 2, as well as their vibration modes were performed utilizing hybrid CAM-B3LYP functional for small atoms like C, H, N, O and LANL2DZ functional for atoms with higher atomic number like Cu. CAM-B3LYP functional was considered instead of B3LYP as significant charge transfer character were involved for the case of metal complex. We have used 6-311G(d,p) basis set for all the atoms, which provides highly precise results on moderate time scale. The electrostatic potential (ESP), total electron density (ED), and frontier molecular orbitals (FMOs) were also studied using the DFT level by means of the B3LYP functional, to obtain adequate information about the electronic characteristics.

Acknowledgements

Authors are grateful to the SAIF Panjab University, SAIF IISER Bhopal for the analysis of the samples and to NTU, Singapore for the single crystal X-ray structure determination. Samaresh Layek and Bhumika Agrahari acknowledges the receipt of IIT (ISM) senior research fellowship.

Appendix A. Supplementary data

Supplementary data to this article can be found online at https://doi.org/10.1016/j.jorganchem.2019.06.008.

References

[1] (a) M.B. Gawande, A. Goswami, F.X. Felpin, T. Asefa, X. Huang, R. Silva, X. Zou, R. Zboril, R.S. Varma, Chem. Rev. 116 (2016) 3722;
(b) M.M. Conejo, J. Cantero, A. Pastor, E. Alvarez, A. Galindo, Inorg. Chim. Acta 470 (2018) 113.
[2] (a) K. Kiranmai, Y. Prashanthi, N. Subhashini, J. Chem. Pharm. Res. 2 (2010) 375;
(b) A. Warra, J. Chem. Pharm. Res. 3 (2011) 951;
(c) M. Padmaja, J. Pragathi, C.G. Kumari, J. Chem. Pharm. Res. 3 (2011) 602.
[3] K. Tummalapalli, V.C.S.P. Munusami, M. Pathak, M.M. Balamurali, Appl. Organomet. Chem. 31 (2016) 3680.
[4] S.E. Allen, R.R. Walvoord, R. Padilla-Salinas, M.C. Kozlowski, Chem. Rev. 113 (2013) 6234.
[5] S.N. Zhao, X.Z. Song, S.Y. Song, H. Zhang, Coord. Chem. Rev. 337 (2017) 80.
[6] (a) X. Tang, W. Wu, W. Zeng, H. Jiang, Acc. Chem. Res. 51 (2018) 1092;
(b) N. Panda, A.K. Jena, Org. Chem. Curr. Res. 4 (2015) 1.
[7] (a) A. Sujatha, A.M. Thomas, A.P. Thankachan, G. Anil Kumar, ARKIVOC (2015) 1;
(b) F. Theil, Angew. Chem. Int. Ed. 38 (1999) 2345;
(c) C.M. Rayner, Contemp. Org. Synth. 3 (1996) 499.
[8] (a) S. Roy, P. Phukan, Tetrahedron Lett. 56 (2015) 2426;
b) L. Li, Y. Ding, Min. Rev. Org. Chem. (2017) 14;
(c) V. Saini, B. Khungar, New J. Chem. 42 (2018) 12796.
[9] (a) A.K. Yudin, J.F. Hartwig, Catalyzed Carbon-Heteroatom Bond Formation, Wiley-VCH, Weinheim, 2010;

(b) H.J. Xu, Y.Q. Zhao, T. Feng, Y.S. Feng, J. Org. Chem. 77 (2012) 2878;
(c) E.M. Beccalli, G. Broggini, M. Martinelli, S. Sottocornola, Chem. Rev. 107 (2007) 5318;
(d) F. Monnier, M. Taillefer, Angew. Chem. Int. Ed. 48 (2009) 6954.
[10] (a) J.E. Anthony, Chem. Rev. 106 (2006) 5028;
(b) T. Mori, T. Nishimura, T. Yamamoto, L. Doi, E. Miyazaki, I. Osaka, K. Takimiya, J. Am. Chem. Soc. 135 (2013) 13900;
(c) P.S. Herradura, K.A. Pendola, R.K. Guy, Org. Lett. 2 (2000) 2019;
(d) P. Saravanan, P. Anbarasan, Org. Lett. 16 (2014) 848.
[11] (a) G. Bastug, S.P. Nolan, J. Org. Chem. 78 (2013) 9303;
(b) A. Thuillier, P. Metzner, Sulfur Reagents in Organic Synthesis, Academic Press, New York, 1994;
(c) A.J. Caruso, A.M. Colley, G.L. Bryant, J. Org. Chem. 56 (1991) 862;
(d) J. Ham, I. Yang, H. Kang, J. Org. Chem. 69 (2004) 3236;
(e) F. Ullmann, P. Sponagel, Ber. Dtsch. Chem. Ges. 38 (1905) 2211;
(f) M. Murata, S.L. Buchwald, Tetrahedron 60 (2004) 7397.
[12] (a) A. Correa, M. Carril, C. Bolm, Angew. Chem. Int. Ed. 47 (2008) 2880;
(b) V.P. Reddy, K. Swapna, A.V. Kumar, K.R. Rao, J. Org. Chem. 74 (2009) 3189;
(c) P. Guan, C. Cao, Y. Liu, Y. Li, P. He, Q. Chen, G. Liu, Y. Shi, Tetrahedron Lett. 53 (2012) 5987;
d) A. Byeun, K. Baek, M.S. Han, S. Lee, Tetrahedron Lett. 54 (2013) 6712;
(e) J. Mondal, A. Modak, A. Dutta, A. Bhaumik, Dalton Trans. 40 (2011) 5228;
(f) W.K. Huang, W.T. Chen, I.J. Hsu, C.C. Han, S.G. Shyu, RSC Adv. 7 (2017) 4912;
(g) C. Lai, H. Kao, Y. Wang, C. Lee, Tetrahedron Lett. 53 (2012) 4365;
(h) C.F. Lee, Y.C. Liu, S.S. Badsara, Chem. Asian J. 9 (2014) 706;
(i) Y. Wong, T.T. Jayanth, C. Cheng, Org. Lett. 8 (2006) 5613;
(j) E. Alvaro, J.F. Hartwig, J. Am. Chem. Soc. 131 (2009) 7858;
(k) F. Luo, C. Pan, L.P. Li, F. Chen, J. Cheng, Chem. Commun. 47 (2011) 5304;
(l) G.T. Venkanna, H.D. Arman, Z.J. Tonzetich, ACS Catal. 4 (2014) 2941;
(m) S.N. Murthy, B. Madhav, V.P. Reddy, Y.V.D. Nageswar, Eur. J. Org. Chem. 34 (2009) 5902;
(n) S. Mallick, S. Rana, K. Parida, Dalton Trans. 40 (2011) 9169;
(o) J. Zhang, C.M. Medley, J.A. Krause, H. Guan, Organometallics 29 (2010) 6393;
(p) O.B. Pantaleon, S.H. Ortega, D.M. Morales, Adv. Synth. Catal. 348 (2006) 236;
(q) V.P. Reddy, A.V. Kumar, K. Swapna, K.R. Rao, Org. Lett. 11 (2009) 1697;
(r) S. Jammi, P. Barua, L. Rout, P. Saha, T. Punniyamurthy, Tetrahedron Lett. 49 (2008) 1484;
(s) F.J. Guo, J. Sun, Z.Q. Xu, F.E. Kühn, S.L. Zang, M.D. Zhou, Catal. Commun. 96 (2017) 11.
[13] R.B. Nasir Baig, R.S. Varma, Chem. Commun. 48 (2012) 2582.
[14] J.V. Faria, M. Silva dos Santos, P.F. Vegi, J.C. Borges, A.M.R. Bernardino, Tetrahedron Lett. 54 (2013) 5748.
[15] U.B. Patil, K.R. Kumthekar, J.M. Nagarkar, Tetrahedron Lett. 53 (2012) 3706.
[16] (a) V.A. Ostrovskii, G.I. Koldobskii, R.E. Trifonov, Comprehensive Heterocyclic Chemistry III, vol. 6, Elsevier, Oxford, 2008, p. 257;
(b) M. Khanmoradi, M. Nikoorajam, A.G. Choghamarani, Appl. Organomet. Chem. 31 (2017) 3693.
[17] P. Moradi, A.G. Choghamarani, Appl. Organomet. Chem. 31 (2016) 1.
[18] S. Layek Anuradha, B. Agrahari, D.D. Pathak, Chem. Select 2 (2017) 6865.
[19] A. Hantzsch, A. Vagt, Justus Liebigs Ann. Chem. 314 (1901) 339.
[20] (a) B. Sreedhar, A.S. Kumar, D. Yadav, Tetrahedron Lett. 52 (2011) 3565;
(b) T. Jin, K.S. Kitahara, Y. Yamamoto, Tetrahedron Lett. 49 (2008) 2824.
[21] V. Rama, K. Kanagaraj, K. Pitchumani, J. Org. Chem. 76 (2011) 9090.
[22] A. Kumar, R. Narayanan, H. Shechter, J. Org. Chem. 61 (1996) 4462.
[23] J. Bonnamour, C. Bolm, Chem. Eur J. 15 (2009) 4543.
[24] G. Venkateshwarlu, A. Premalatha, K.C. Rajanna, P.K. Saiprakash, Synth. Commun. 39 (2009) 4479.
[25] D.P. Matthews, J.E. Green, A.J. Shuker, J. Comb. Chem. 2 (2000) 19.
[26] M.L. Kantam, K.B. Shiva Kumar, C. Sridhar, Adv. Synth. Catal. 347 (2005) 1212.
[27] G. Baskaya, I. Esirden, E. Erken, F. Sen, M. Kaya, J. Nanosci. Nanotechnol. 17 (2017) 1992.
[28] L. Lang, B. Li, W. Liu, Li Jiang, Z. Xu, G. Yin, Chem. Commun. 46 (2010) 448.
[29] S. Layek, R. Ganguly, D.D. Pathak, J. Organomet. Chem. 870 (2018) 16.
[30] (a) Y. Yıldız, I. Esirden, E. Erken, E. Demir, M. Kaya, F. Sen, Chem. Select 1 (2016) 1695;
(b) P. Moradi, A.G. Choghamarani, Appl. Organomet. Chem. 31 (2016) 3602;
(c) M. Nikoorazm, A.G. Choghamarani, M. Ghobadi, S. Massahi, Appl. Organomet. Chem. 31 (2017) 3848;
(d) I. Esirdena, E. Erken, M. Kaya, F. Sen, Catal. Sci. Technol. 5 (2015) 4452;
(e) E. Erken, I. Esirden, M. Kaya, F. Sen, RSC Adv. 5 (2015) 68558.
[31] (a) C. Tao, B. Wang, L. Sun, J. Yi, D. Shi, J. Wang, W. Liu, J. Chem. Res. 41 (2016) 25;
(b) M.M. Heravi, A. Fazeli, H.A. Oskooie, Y.S. Beheshtiha, H. Valizadeh, Synlett 23 (2012) 2927;
(c) M.A. Alibeik, A. Moaddeli, New J. Chem. 39 (2015) 2116;
(d) S. Behrouz, J. Saudi. Chem. Soc. 21 (2017) 220.
[32] (a) S. Layek, S. Kumari, Anuradha, B. Agrahari, R. Ganguly, D.D. Pathak, Inorg. Chim. Acta 453 (2016) 735;
(b) S. Layek, Anuradha, B. Agrahari, D.D. Pathak, J. Organomet. Chem. 846 (2017) 105;
(c) S. Layek, B. Agrahari, A. Tarafdar, C. Kumari, Anuradha, R. Ganguly, D.D. Pathak, J. Mol. Struct. 1141 (2017) 428;
(d) B. Agrahari, S. Layek, Anuradha, R. Ganguly, D.D. Pathak, Inorg. Chim. Acta 471 (2017) 345;
(e) S. Kumari Anuradha, S. Layek, D.D. Pathak, New J. Chem. 41 (2017) 5595;
(f) B. Agrahari, S. Layek, S. Kumari, Anuradha, R. Ganguly, D.D. Pathak, J. Mol. Struct. 1134 (2017) 85;
(g) S. Layek, B. Agrahari, S. Kumari, Anuradha, D.D. Pathak, Catal. Lett. 148 (2018) 2675;
(h) B. Agrahari, S. Layek, R. Ganguly, N. Dege, D.D. Pathak, J. Organomet. Chem. 890 (2019) 13.
[33] T. Maity, D. Saha, S. Koner, ChemCatChem 6 (2014) 2373.
[34] B.N. Bessy Raj, M.R.P. Kurup Spectrochim, Acta, Part A 66 (2007) 898.
[35] B. Agrahari, S. Layek, R. Ganguly, D.D. Pathak, New J. Chem. 42 (2018) 13754.
[36] K. Tummalapalli, C.S. Vasavi, P. Munusami, M. Pathak, M.M. Balamurali, Appl. Organomet. Chem. 31 (2017) 3680.
[37] K. Venkateswarlu, M.P. Kumar, A. Rambabu, N. Vamsikrishna, S. Daravath, K. Rangan, Shivaraj, J. Mol. Struct. 1160 (2018) 198.
[38] (a) K. Majee, J. Patel, B. Das, S.K. Padhi, Dalton Trans. 46 (2017) 14869;
(b) J. Cheng, K. Wei, X. Ma, X. Zhou, H. Xiang, J. Phys. Chem. C 117 (2013) 16552;
(c) P. Zivec, F. Perdih, I. Turel, G. Giester, G. Psomas, J. Inorg. Biochem. 117 (2012) 35.
[39] (a) X. Dong, Y. Li, Z. Li, Y. Cui, H. Zhu, J. Inorg. Biochem. 108 (2012) 22;
(b) M.P. Kumar, S. Tejaswi, A. Rambabu, V. Kumar, A. Kalalbandi, Shivaraj, Polyhedron 102 (2015) 111.
[40] (a) M. Kazemnejadi, A.R. Sardarian, RSC Adv. 6 (2016) 91999;
(b) B. Mitra, S. Mukherjee, G.C. Pariyar, P. Ghosh, Tetrahedron Lett. 59 (2018) 1385.
[41] S.H. Lee, N. Shin, S.W. Kwak, K. Hyun, W.H. Woo, J.H. Lee, H. Hwang, M. Kim, J. Lee, Y. Kim, K.M. Lee, M.H. Park, Inorg. Chem. 56 (2017) 2621.
[42] (a) O. Prakash, K.N. Sharma, H. Joshi, P.L. Gupta, A.K. Singh, Organometallics 33 (2014) 2535;
(b) F. Saleem, G.K. Rao, A. Kumar, S. Kumar, M.P. Singh, A.K. Singh, RSC Adv. 4 (2014) 56102.
[43] T.P. Chiu, S. Rao, R.S. Mann, B. Honig, R. Rohs, Nucleic Acids Res. 45 (2017) 12565.
[44] F. Zhang, B. Liu, G. Liu, Y. Zhang, J. Wang, S. Wang, Sci. Rep. 8 (2018) 3131.
[45] SMART Version 5.628, Bruker AXS Inc., Madison, WI, USA, 2001.
[46] G. Sheldrick, M. SADABS, University of Göttingen, Göttingen, 1996. Germany.
[47] SHELXTL Version 5.1, Bruker AXS Inc., Madison, WI, USA, 1997.